Liebau Pumping Enables Valveless Soft Swimmer Robot

Gabriel Unger[1], Saheli Patel[1], Benjamin Kozyak[2], Jordan R. Raney[1], and Cynthia Sung[1]

[1] University of Pennsylvania, Philadelphia, PA, USA 19104
{gunge1,spatel99,raney,crsung}@seas.upenn.edu
[2] Children's Hospital of Philadelphia, Philadelphia, PA, USA 19104
kozyakbw@chop.edu

Abstract. Liebau pumping produces net directional flow via periodic compression of a compliant tube at an asymmetric location, eliminating the need for valves or check flaps. While attractive for its simplicity, this mechanism has rarely been explored for robotic propulsion. Here, we present the first free-swimming robot actuated solely by Liebau pumping. A soft silicone conduit is cyclically compressed off-center by a single solenoid actuator, generating traveling pressure waves that produce thrust. Directional control is achieved through simple frequency switching, enabling both forward and reverse swimming. Experimental results reveal distinct frequency bands that correspond to the forward and reverse swimming modes, with peak velocities of 5.25 cm/s forward at 11 Hz and –1.58 cm/s in reverse at 15 Hz using a 30% duty cycle and 1 A peak current. Agility tests confirm smooth, responsive transitions between directions without mechanical valves or moving parts. These results establish Liebau pumping as a viable, low-complexity propulsion method for soft and ecologically safe underwater robots.

Keywords: soft robots, valveless pumping, Liebau effect, bidirectional propulsion, underwater robotics

1 Introduction

Small, low-cost underwater robots offer promising solutions for environmental monitoring in sensitive aquatic habitats [1]. However, traditional propeller-based designs can pose hazards to marine life by causing entanglement or injury and generating noise that may disturb underwater ecosystems [2]. Alternative propulsion systems range from fin-based swimming, modeled after fish [3], to jet propulsion inspired by squids and jellies [4, 5]. While fin-based methods can provide higher speeds and agile maneuvering [6], underwater jetting approaches can exhibit simpler mechanical designs and lower cost of transport (CoT) [4]. However, both swimming modes are often limited to forward motion, and adding backwards swimming requires additional mechanisms such as valves.

Background on Liebau Pumping This work investigates the Liebau mechanism, a valveless pumping principle first observed in embryonic heart function [7], as a method for enabling bidirectional underwater robotic propulsion. Liebau pumping operates through asymmetric, oscillatory compression of a compliant tube, generating traveling waves that induce a net flow without valves or check flaps. Originally described by Liebau in the 1950s [8, 9], the mechanism has been widely studied in theoretical models and bench-top experimental settings [10, 11]. However, most studies have been limited to closed-loop fluidic circuits, and real-world applications have been constrained by the system's nonlinear dynamics: small changes in actuation frequency, compression amplitude, or compression location can dramatically alter both the direction and magnitude of flow [10, 12, 13]. Most prior work has focused on isolated parameters rather than interactions among variables or their effects on fully integrated mechanical devices. Further, Liebau pumping has not been demonstrated in free-swimming robots.

Contributions Here, we extend Liebau pumping beyond closed-loop setups by embedding it into a free-swimming robotic platform, demonstrating that short compliant tubes can generate thrust in open-water environments for forward and reverse propulsion. This robotic implementation eliminates traditional propellers and valves, offering a simpler and potentially safer alternative for navigation in debris-laden or sensitive aquatic environments. We systematically investigate how key actuation parameters, specifically frequency, duty cycle, and compression force, affect swimming speed and direction, focusing on tuning the system for bidirectional locomotion. Rather than conducting a full energy analysis, we centered our study on identifying how these parameters influence thrust magnitude and direction. By embedding the Liebau effect into an underwater robot, we contribute (1) a *robotic integration* of Liebau valveless pumping and (2) a *systematic mapping* of the propulsion response across key actuation parameters. To our knowledge, this is the first demonstration of a valveless pumping mechanism achieving sustained, bidirectional swimming in a free-swimming robotic system.

2 System Design and Experimental Setup

Our robotic swimmer (Fig. 1) centers around a soft, valveless pumping unit inspired by the Liebau mechanism. Key to this mechanism are two features that enable valveless propulsion: (1) off-center compression of a compliant tube, and (2) the impedance mismatch at the soft–rigid interfaces at the ends of the tube. Combined, these features generate traveling pressure waves. To create these conditions, we construct the robot as a 150 mm long silicone conduit fabricated from Ecoflex 00-30, with an outer diameter of 16 mm and a wall thickness of 2 mm. Hose barb clamps (McMaster-Carr #5372K516) are inserted into each end of the soft tube to create rigid internal interfaces that provide the impedance mismatch necessary for wave reflection. Because Ecoflex is too flexible to hold the clamps securely on its own, rigid polyurethane connectors (McMaster #5236K518) are

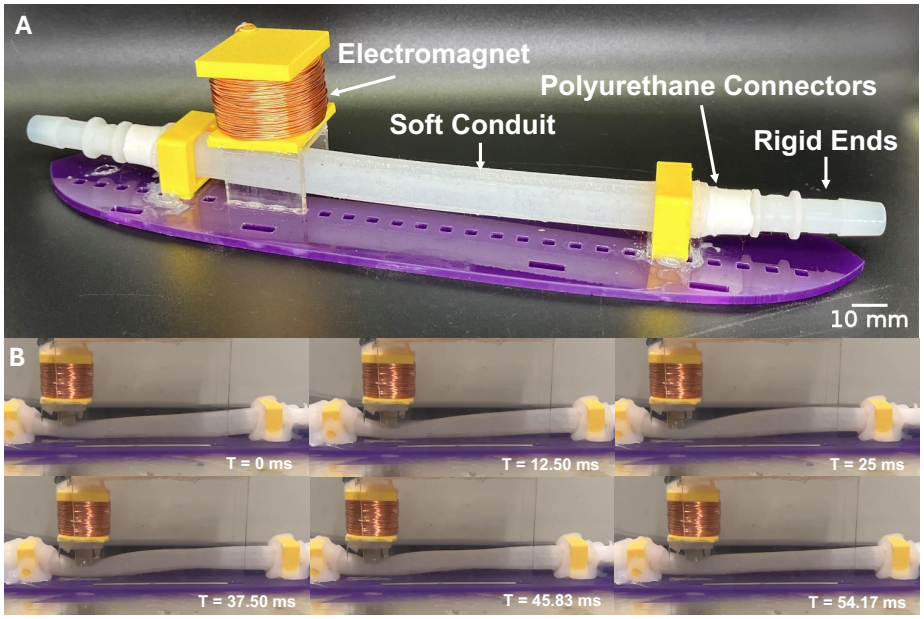

Fig. 1. (A) Fabricated swimmer robot showing the Ecoflex conduit (soft tubing), hose barb clamps inserted at each end to establish rigid internal interfaces for wave impedance, and polyurethane connectors bonded externally to anchor the clamps and provide mechanical support. (B) High-speed (240 FPS) snapshots of one full underwater actuation sequence at 11 Hz with 30% duty cycle, showing a traveling wave essential for propulsion.

bonded around the outside of each tube end using Sil-Poxy adhesive. These connectors mechanically anchor the hose barb clamps and prevent detachment or deformation during actuation. Both components sit at the conduit–connector junction, but they serve different roles. The hose-barb clamps create the internal rigid boundaries that generate wave impedance, whereas the polyurethane connectors add external reinforcement that keeps the clamps from shifting or detaching during actuation. A custom electromagnetic actuator provides the periodic asymmetric compression required for Liebau pumping. The actuator consists of a neodymium magnet core ($\frac{1}{2}'' \times \frac{3}{8}'' \times \frac{5}{4}''$) surrounded by 300 turns of copper wire. Positioned laterally against the tube, the actuator pinches the conduit off-center, producing the necessary asymmetry for effective pumping. The actuator is driven by a 30 V, 5 A power source controlled via an Arduino Uno micro-controller interfaced with a Hilitand 4-Channel MOSFET motor driver. This setup enables precise control of actuation frequency (0-20 Hz), duty cycle (0-100%), and compression force (modulated via current). The actuation assembly and conduit are mounted beneath a neutral-buoyancy float, ensuring the robot remains fully submerged during operation.

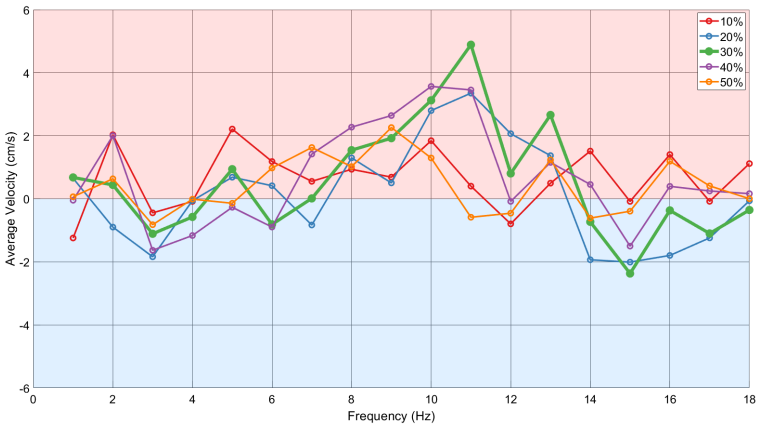

Fig. 2. Average swimming velocity versus actuation frequency at varying duty cycles with a 1 A peak, square wave input. Distinct forward and reverse propulsion bands emerge, with peak forward velocities at 11 Hz and peak reverse velocities at 15 Hz. Duty cycle influences conduit refill time, modulating thrust amplitude and band location. Line colors indicate duty cycle percentage. Red and blue background shading denote regions of positive and negative average velocity, respectively.

To track the robot's motion during experiments, five reflective markers were placed on the robot's buoyancy float. Experiments were conducted in a 115 cm × 230 cm × 26 cm (L × W × H) water tank. A ceiling-mounted OptiTrack motion-capture system recorded the robot's pose at 120 Hz, while simultaneous coil-voltage and current logs were collected to monitor electrical power input. The assembled robot was tethered during testing for power delivery and motion capture but was otherwise free-swimming within the tank environment. With this setup, we systematically varied actuation parameters (frequency, duty cycle, and compression force) to investigate their effects on swimming performance, focusing on tuning the system for controlled forward and backward locomotion. By holding the robot geometry and material properties constant, we isolated how these parameters drove thrust generation and bidirectional swimming.

3 Experimental Results

3.1 Combined Effects of Actuation Frequency and Duty Cycle

To characterize the propulsion performance of the swimmer robot, we first systematically varied the actuation frequency from 0 Hz to 20 Hz in 1 Hz increments while maintaining a fixed actuation amplitude of 1 A and a 50% duty cycle. For each trial, we captured pose data with the motion-capture system. The x, z, and yaw components were extracted, then filtered and smoothed using a moving average filter and a low-pass filter to remove high-frequency noise. Velocity was

then computed by taking the numerical derivative of the filtered position signals over time and projecting the result into the heading direction of the robot. Occasional orientation artifacts in the pose data were manually identified and corrected using linear interpolation to ensure continuity. The average velocity for each frequency was calculated over a manually selected observation window corresponding to steady-state motion, typically beginning after the initial acceleration phase and ending before the robot reached the edge of the tank.

Fig. 2 shows the resulting velocity profile as a function of frequency. As the actuation frequency is swept, distinct forward and reverse propulsion bands emerge, with the flow direction switching as frequency increases, which is a hallmark of Liebau-type pumping. Qualitative observations of these initial sweeps revealed that incomplete refill of the conduit limited thrust. That is, at high frequencies, the compliant tube was not able to return to its fully expanded state, reducing overall fluid flow.

To investigate whether increasing the refill time could improve performance, we additionally varied the actuation duty cycle from 10% to 50% in 10% increments. For each duty cycle setting, we repeated the same frequency sweep from 0 Hz to 18 Hz in 1 Hz increments while maintaining a constant actuation amplitude of 1 A. Frequencies above 18 Hz were excluded because preliminary trials showed no measurable net displacement at higher actuation rates. Duty cycles above 50% were not explored because, based on experimental observations, high duty cycles reduced the refill time of the conduit, which further limit thrust generation. Since the objective of this study was to increase refill time and assess its effect on propulsion, we focused exclusively on lower duty cycles that favor longer refill periods. In addition, we would expect longer duty cycles to be energetically unfavorable, increasing energy consumption without a corresponding performance benefit. This approach allowed us to assess how refill dynamics influenced propulsion across the full frequency range.

Results, summarized in Fig. 2, showed two strong forward-propulsion bands, with peak performance at 11 Hz, and a prominent reverse-propulsion band centered around 15 Hz. A 30% duty cycle performed best for both cases, likely because reducing the duty cycle improved conduit refill between compressions, leading to stronger and more consistent thrust generation. Based on these observations, we selected a 30% duty cycle as an optimal trade-off between thrust performance and energy consumption for all subsequent experiments.

As a control, we repeated the frequency sweep after removing the rigid end connectors, leaving only the soft silicone conduit. Under these conditions, no observable net motion was detected across the entire frequency range, underscoring the critical role of impedance mismatch at the soft–rigid interfaces in enabling effective Liebau pumping.

3.2 Effect of Compression Force

To evaluate the influence of compression force on swimming performance, we performed a series of tests varying the peak coil current while holding frequency and duty cycle constant at 11 Hz and 30%, respectively, the optimal forward

Table 1. Mean swimming velocities at different coil currents for single-direction trials, all using a 30% duty cycle. Velocities are reported as mean (standard deviation).

Frequency (Hz)	Current (A)	Velocity (cm/s)
11	0.25	5.27 (0.76)
11	0.50	5.36 (0.67)
11	1.00	5.25 (0.34)
15	1.00	-1.57 (0.33)

propulsion condition identified in prior experiments. We incrementally increased the coil current from 0.25 A to 3 A in steps of approximately 0.1 A and observed the robot's motion in the tank. No noticeable change in swimming speed was observed across the tested current range. To validate these findings, we performed quantitative trials. Trials were conducted at three coil currents (1 A, 0.5 A, and 0.25 A) with three repetitions at each setting. Table 1 summarizes the mean swimming velocities and standard deviations. Overall, increasing the coil current beyond 0.25 A provided no measurable performance benefit but incurred higher power consumption. For consistency with previous experiments, we used a 1 A peak current for subsequent trials; however, these results suggest that lower current levels could be employed without sacrificing swimming performance.

3.3 Bidirectional Control and Agility

Propulsion Forward and Backward The Liebau effect enables bidirectional pumping: in our system, shifting the actuation frequency from the forward resonance band (11 Hz) to the reverse resonance band (15 Hz) inverts the flow direction even while all other parameters are held constant. To quantify this behavior, we conducted three straight-run trials each at 11 Hz and 15 Hz, using a 30% duty cycle and a peak actuation current of 1 A. Across the three forward trials at 11 Hz, the robot achieved a mean maximum velocity of 5.25 cm/s, with a mean forward acceleration of 0.57 cm/s^2. In contrast, the backward trials at 15 Hz produced a mean maximum velocity of -1.57 cm/s and a mean backward acceleration of -0.54 cm/s^2. These results demonstrate that changing the actuation frequency effectively reverses the swimming direction. Notably, the magnitude of the backward speed and acceleration were lower than their forward counterparts, consistent with the asymmetry observed in the frequency sweep experiments and characteristic of the nonlinear flow behavior reported in Liebau-type pumping literature [10, 13].

Direction Changes The robot's agility is limited by its acceleration and its ability to quickly switch its direction of travel. We evaluated the robot's agility through two strategies:

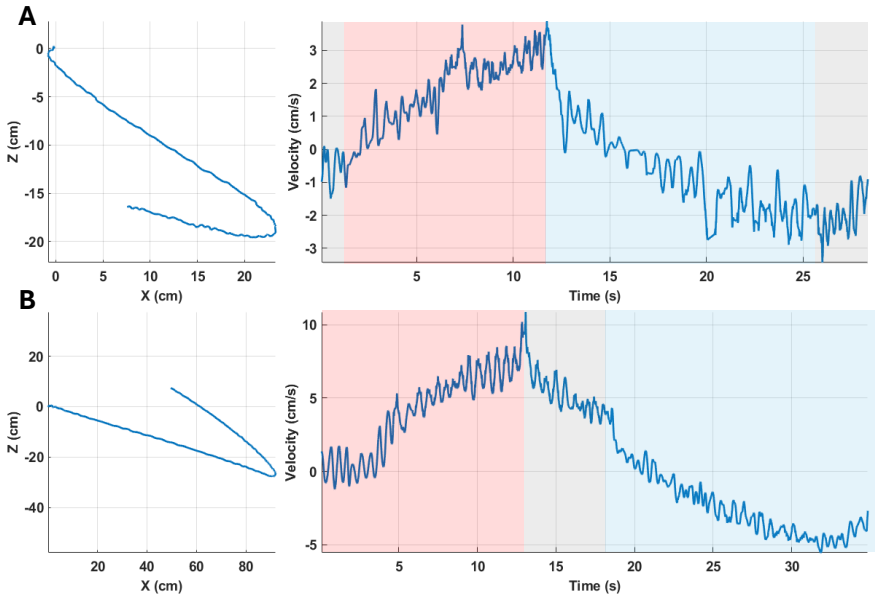

Fig. 3. Trajectory and velocity over time for (A) Forward–Backward (FB) and (B) Forward–Stop–Backward (FSB). Red shading indicates periods when the robot is receiving the forward command (11 Hz, 30% duty cycle), blue shading indicates the reverse command (15 Hz, 30% duty cycle), and grey shading indicates no signal input.

- **Forward–Backward (FB)**: Drive forward at 11 Hz, 30% duty cycle for 10 s, then immediately switch to backward drive at 15 Hz, 30% duty cycle for 15 s without stopping.
- **Forward–Stop–Backward (FSB)**: Drive forward at 11 Hz, 30% duty cycle for 10 s; stop for 5 s; then drive backward at 15 Hz, 30% duty cycle for 15 s.

For each test sequence, the robot was actuated at the prescribed frequency, duty-cycle, and compression-force settings (see Section 2). Its motion was captured with the ceiling-mounted OptiTrack system at 120 Hz. We ran multiple trials of the Forward–Backward (FB) and Forward–Stop–Backward (FSB) maneuvers, logging the robot's 3-D position and computing its velocity as previously described. Fig. 3 presents representative trajectories and velocity profiles: in panels A and B, the left plots show path taken by the robot in the horizontal plane, while the right plots display the corresponding velocity-versus-time curves. Table 2 lists the peak velocities and mean accelerations across all trials, confirming that the robot achieves consistent, responsive bidirectional swimming without valves or external moving parts.

Table 2. Mean accelerations during different driving phases. Accelerations are reported as mean (standard deviation).

Driving Phase	**Forward Acc.** (cm/s^2)	**Backward Acc.** (cm/s^2)
Single Direction	0.57 (0.04)	-0.54 (0.24)
Forward-Backward	0.43 (0.19)	-0.35 (0.03)
Forward-Stop-Backward	0.68 (0.06)	-0.37 (0.12)

4 Discussion

We have demonstrated valveless swimming in a soft robot inspired by Liebau pumping. Our results indicate that this pumping method can be an effective strategy for generating both forward and backward motion with minimal actuation and a simple robot design. Compared to prior Liebau studies, which were carried out in closed-loop test rigs or in circuits that link two reservoirs with a compliant tube [12, 10], our results extend the mechanism to a free-swimming context, where the traveling pressure wave inside the compliant tube couples directly to the surrounding fluid to produce thrust. Because the wave itself is the propulsive agent, the position of the forward and reverse resonant bands depend on both the tube's mechanical properties and the added mass of the external fluid. In examining how actuation parameters affect performance, we observed that increasing compression force beyond a certain threshold led to diminishing returns in swimming speed. This is likely due to nonlinearities in the pressure wave dynamics: once the tube is fully collapsed during compression, applying greater force does not meaningfully increase wave speed or amplitude. These findings suggest that actuation efficiency achieving sufficient deformation with minimal power may be more important than maximizing force output. Beyond steady-state performance, these tests further underscore the potential of Liebau-based propulsion for real-time maneuvering. The Forward–Backward (FB) and Forward–Stop–Backward (FSB) trials demonstrated smooth, consistent directional reversals achieved solely through frequency switching. These transitions occurred without mechanical reconfiguration or latency, validating the use of this system for responsive navigation. Differences in acceleration between the FB and FSB conditions suggest that factors such as fluid inertia and internal flow stabilization influence transition dynamics. These characteristics point toward the viability of Liebau pumping for applications such as obstacle avoidance or station-keeping in cluttered aquatic environments. Together, these results establish valveless Liebau pumping not only as a viable propulsion method but also as one with unique advantages in simplicity, safety, and responsiveness. Continued investigation into wave mechanics, actuator efficiency, and integrated control strategies will further unlock the potential of this biologically inspired mechanism for underwater robotics.

5 Limitations and Future Work

While the present work demonstrates effective valveless propulsion, several opportunities remain to enhance performance and extend system capabilities. First is the tuning of tube mechanics, specifically wall thickness, overall length, the stiffness difference between rigid and soft sections, and actuation footprint. Optimizing these parameters may sharpen the reflection boundary, increasing momentum transfer and propulsion efficiency. Hydrodynamic performance also stands to benefit from improved form factor. The current prototype exposes tubing to crossflow and offsets the actuator from the centerline, contributing to unnecessary drag. A streamlined hull design that integrates the conduit along the centerline could reduce drag, stabilize the swimmer during rapid acceleration, and improve energy efficiency.

A central insight from this study is the tight coupling between hardware and control: swimming direction is not solely dictated by either the mechanical layout or actuation strategy, but by their interplay. Consequently, design should not proceed by independently optimizing geometry and drive signals. Instead, we propose an integrated optimization framework that simultaneously tunes conduit parameters and control waveforms, including frequency, duty cycle, and pressure amplitude. Such a pipeline could reveal new regimes of valveless propulsion, offering trade-offs between speed, controllability, and energy cost. They may also expand the bidirectional swimming range and help to ensure smooth transitions between gaits. In particular, a generalized control architecture capable of detecting local resonance conditions, and adjusting actuation accordingly would allow the robot to adapt to variations stemming from fabrication tolerances, material aging, or environmental shifts. This adaptability is crucial for long-term autonomy.

Finally, at present, actuator efficiency remains a key bottleneck. Our in-house solenoid was chosen for its modularity, but its hydrodynamic profile is suboptimal. Future designs should explore more efficient actuation strategies and geometries that integrate seamlessly with the body.

6 Conclusion

This work demonstrates, for the first time, a free-swimming robot that relies exclusively on Liebau valveless pumping for propulsion. A single off-center solenoid actuator produces bidirectional thrust through simple frequency switching and reaches $5.25\,\mathrm{cm\,s^{-1}}$ in the forward direction and $-1.58\,\mathrm{cm\,s^{-1}}$ in reverse while keeping mechanical complexity low. Although its efficiency still trails that of conventional propeller systems, the study confirms valveless pumping as a safe and robust alternative for soft and ecological robotics. Removing external moving parts and using frequency to reverse direction gives clear advantages when navigating cluttered or delicate aquatic habitats. Future improvements in actuator efficiency, hydrodynamic form, and closed loop resonance control are expected to narrow the performance gap and broaden the practical envelope of Liebau based propulsion.

Acknowledgments

This work was supported in part by the Children's Hospital of Philadelphia (CHOP) through the Cardiac Center Innovation Award Program, Office of Naval Research (ONR) Award #N00014-23-1-2068, and Air Force Office of Scientific Research (AFOSR) Award #FA9550-23-1-0299. The authors would also like to thank Louis Beardell and Serena Carson for their assistance with fabrication, and Kayleen Smith for help with the motion capture setup.

References

1. Maslin, M., Louis, S., Godary Dejean, K., Lapierre, L., Villéger, S., Claverie, T.: Underwater robots provide similar fish biodiversity assessments as divers on coral reefs. Remote Sensing in Ecology and Conservation 7(4), 567–578 (2021)
2. Wilson, B., Batty, R.S., Daunt, F., Carter, C.: Collision risks between marine renewable energy devices and mammals, fish and diving birds. Report to the scottish executive, Scottish Association for Marine Science, Oban, Scotland, PA37 1QA (2006)
3. Sfakiotakis, M., Lane, D.M., Davies, J.B.C.: Review of fish swimming modes for aquatic locomotion. IEEE Journal of Oceanic Engineering 24, 237–252 (1999)
4. Yang, Z., Chen, D., Levine, D.J., Sung, C.: Origami-inspired robot that swims via jet propulsion. IEEE Robotics and Automation Letters 6(4), 7145–7152 (2021)
5. Yang, Z., Zhang, Y., Herbert, M., Hsieh, M.A., Sung, C.: Effect of jet coordination on underwater propulsion with the multi-robot salp system. In: 8th IEEE-RAS International Conference on Soft Robotics (RoboSoft 2025) (2025)
6. Palmisano, J.S., Geder, J.D., Pruessner, M.D., Ramamurti, R.: Power and thrust comparison of bio-mimetic pectoral fins with traditional propeller-based thrusters. Tech. rep., Naval Research Laboratory, Washington, DC, USA (2014)
7. Forouhar, A., Liebling, M., Hickerson, A., Nasiraei-Moghaddam, A., Tsai, H., Hove, J., et al.: The embryonic vertebrate heart tube is a dynamic suction pump. Science 312, 751–753 (2006)
8. Liebau, G.: Principles of blood circulation of the heart. Z. Kreislaufforsch. 44(17-18), 677–684 (Sep 1955)
9. Liebau, G.: Heart beat and blood movement. Z. Gesamte Exp. Med. 125(5), 482–498 (1955)
10. Meier, R.: Valveless impedance pumping at the microscale: Experimental and theoretical studies. Ph.D. thesis, ETH Zurich (2011)
11. Anatol, J., García-Díaz, M., Barrios-Collado, C., Moneo-Fernández, J.A., Rubio, M., Castro-Ruiz, F., Sierra-Pallares, J.: An assessment of the suitability of a liebau pump in biomedical applications. Physics of Fluids 36(1) (2024)
12. Hickerson, A., Gharib, M.: Experimental study of the behavior of a valveless impedance pump. Journal of Fluid Mechanics 555, 141–148 (2005)
13. Hiermeier, F., Männer, J.: Kinking and torsion can significantly improve the efficiency of valveless pumping in periodically compressed tubular conduits. implications for understanding of the form-function relationship of embryonic heart tubes. Journal of Cardiovascular Development and Disease 4(4), 19 (2017)